J. Chem. Sci. (2021)133:104
https://doi.org/10.1007/s12039-021-01973-8

REGULAR ARTICLE

Dielectric relaxations of molten acetamide: dependence on the model interaction potentials and the effects of system size

DHRUBAJYOTI MAJI[a], SANDIPA INDRA[b] and RANJIT BISWAS[a,*]
[a]Chemical, Biological and Macromolecular Sciences, S. N. Bose National Centre for Basic Sciences, Block-JD, Sector-III, Salt Lake, Kolkata, West Bengal 700106, India
[b]Department of Chemistry, Indian Institute of Technology Patna, Bihar 801106, India
E-mail: ranjit@bose.res.in

MS received 6 May 2021; revised 25 June 2021; accepted 29 June 2021

Abstract. Molecular dynamics simulations of dielectric relaxations (DRs) in neat molten acetamide (CH_3CONH_2) at ~358 K have been carried out by employing two different versions of the OPLS force field parameters, namely, the OPLS-UA (united-atom) and the OPLS-AA (all-atom) model interactions. Three systems consisting of 250, 500, and 1000 molecules have been studied to examine the impact of system size on the simulated dielectric properties. A comparison between our simulation predictions and the experimental DR data in the MHz-GHz frequency regime reveals that the OPLS-UA interaction parameters better reproduce the experimental static dielectric constant, whereas the OPLS-AA interaction describes well the measured DR time constants. Moreover, a weak system size dependence has been observed. A Cole-Cole plot of the simulated and experimental dielectric spectra reveal non-Debye nature of liquid acetamide and corroborates well with the earlier observation on the collective single-particle reorientational relaxation of liquid acetamide. The simulated single dipole reorientation dynamics also reflects this weak non-Debye nature and reveals its contribution to the collective polarization relaxation. Simulation results obtained here set the right ground for investigating the colossal dielectric constant (~10^6) of ionic acetamide deep eutectics reported earlier *via* DR measurements in the KHz-MHz regime.

Keywords. Molecular dynamics simulation; dielectric properties; molten acetamide.

1. Introduction

Amide systems are an interesting class of molecules because of their proximity to the world of proteins and peptides in terms of functional groups.[1,2] The existence of the peptide bond (-CO-NH-) in amides which is also the linkage unit in polypeptides and proteins makes amides biologically relevant. Acetamide (CH_3CONH_2) is the smallest amide that contains a methyl group and participates in hydrogen bonding *via* two amide hydrogens and one carbonyl oxygen.[3–5] As a result, acetamide offers a simple molecular model for studying the effects of hydrogen bonding in peptide and amino acids. This assumes further importance given that the structure and function of a protein are dictated by H-bond interactions. Moreover, liquid acetamide is a useful solvent for its high polarity (static dielectric constant, $\varepsilon_s \sim 65$) and low viscosity (~2.2 cP).[6–10] Therefore, several studies have been performed on acetamide and other small amides.[11–18] In recent years, deep eutectic solvents (DESs) have arrived as better alternatives to conventional organic solvents. Several studies have already explored the dynamics of acetamide in DESs that contain acetamide as one of the main components.[19–27] The orientation jump mechanism and its connection to H-bond dynamics, established for water reorientation dynamics,[28,29] has been investigated for molten acetamide as well.[19,25] Recently, dielectric relaxation measurements of neat molten liquid acetamide in the frequency window, $0.2 \leq \nu/GHz \leq 50$, have been reported for the first time.[26] In contrast, no simulation study on DR of in neat, molten acetamide has been performed yet.

*For correspondence
Supplementary Information: The online version contains supplementary material available at https://doi.org/10.1007/s12039-021-01973-8.

Published online: 13 September 2021

Extensive simulation study of neat liquid acetamide examining several aspects, such as influence of model interaction potential, simulation run time and simulation system size dependencies are required to understand the impact of other species on the structure and dynamics of acetamide in a deep eutectic system. Often electrolytes and other neutral compounds are mixed with acetamide to prepare room temperature deep eutectic solvents to explore possibilities for applications as synthesis media. Several studies of ionic acetamide deep eutectics have been carried out in the past to characterize the relaxation behaviour of acetamide in those media and to deduce, *via* interpretation of the measured relaxation parameters, the collective structure of acetamide at that solution condition.[30–34] One of the spectacular yet the most debatable finding of those studies has been the mega value ($\sim 10^6$) of the ε_s of ionic acetamide DESs determined *via* DR measurements employing a KHz-MHz frequency window.[30,33,34] Although a low-frequency divergence swamps the dielectric response of conducting solutions as the frequency of the applied electric field approaches zero, the correct value of ε_s must be accessed to understand the ion influence on the macroscopic polarization response of a neat dipolar system. Considering the difficulty of DR measurements for conducting solutions in attaining the plateau for the real part of the complex dielectric spectra in the limit of zero frequency, one can resort to computer simulations where the ionic and non-ionic contributions to the total polarization response could be easily separated and understood. This separation is critical to examine whether the colossal ε_s of ionic acetamide DESs reported in earlier DR measurements[30,33,34] is at all real or an experimental artefact due to electrode polarisation.

However, computer simulations with classical interaction potentials have their limitations too. The most critical of them is the availability of the appropriately coarse-grained classical interaction potentials that can reproduce the experimentally measured structural and dynamical quantities. It has been found in many cases, particularly for solvents participating in an extensive inter-and intra-molecular H-bonding, that the designed model interaction potentials are unable to simultaneously predict the experimentally observed structural and dynamical properties. In such cases, the choice of interaction potential depends on the final goal of the planned study. This means that if properties regulated by the spatial arrangements of medium particles are to be investigated then the interaction parameters that better predict the solvent structural aspects are employed. For a focus on reproducing the relaxation timescales (for example, diffusion and conductivity timescales), potential parameters that are designed to provide a good description of the collective dynamics are used. Although solvent structure represents the spatial particle arrangements arising from averaging the faster changes (fluctuations) over a certain duration (and thus a function of the averaging timescale), model interaction parameters designed to reproduce solvent dynamics cannot always successfully predict the structural properties. This is a limitation that is a direct consequence of describing collective interactions in terms of classical pair potentials and no explicit treatment of polarizabilities, a trade-off between the quantitative description of the experimental properties and a judicious choice of accessing the computational resources for gaining a qualitatively correct molecular-level understanding of the observed phenomena. Temperature transferability and the applicability of a set of potential parameters developed for a neat system to describe interactions in a multicomponent mixture are other critical issues that prevent quantitative interpretation of the simulation results.

In such a scenario, simulation study of molten acetamide demands careful consideration of the following aspects: (i) If one of the central foci of a planned study is to examine the mega-value of ε_s of ionic acetamide deep eutectics, then one must start with a model interaction potential that has been designed to reproduce the experimental ε_s of neat molten acetamide, (ii) system size of such simulations must be appropriately decided upon as ε_s is a collective solvent property and connected to the macroscopic (that is, large wavelength) solvent polarisation fluctuations, and (iii) a parallel simulation study must be carried out with another set of interaction potential parameters that have been developed to better describe the relaxation timescales. A judicious juxtaposition of the simulation data obtained *via* employing these two different sets of model potentials may then provide a qualitatively correct picture of the collective orientational polarisation relaxations of such ionic media. This provides the basic premises for our present study.

Here we present molecular dynamics simulations of neat molten acetamide at 358.15 K and report results with an aim to interpret the experimentally available DR data. We have considered two different models of interaction potentials based on the optimised potential for liquid simulations (OPLS) force fields. They are the united-atom (OPLS-UA)[35] and the all-atom (OPLS-AA)[36] interaction potentials. Interestingly, the OPLS-UA model[35] predicts a value of ε_s for molten acetamide that agrees quite well with that reported in

experiments[37] but predicts a DR dynamic that is ~3 times slower than found in the relevant experiments. The OPLS-AA model interaction parameters,[36] in contrast, provides a much better description of the experimental DR dynamics but severely underestimates the ε_s value. To check the impact of system size we have also performed simulations on three systems with 250, 500, and 1000 numbers of molecules. A direct comparison between the simulated and experimental dielectric response for neat molten acetamide has been presented and the role of single dipole rotation explored.

2. Theory and computational details

2.1 *Theory*

The dielectric spectrum of a polar system can be calculated by using the total dipole moment of the system. In a polarizable model, electronic polarizability is explicitly considered but at the expense of high computational efficiency. A non-polarizable model deliberately omits the electronic polarizability and set the dielectric function at a high frequency (theoretically infinite) (ε_∞) to unity. Static dielectric constant (ε_s) is the value of the frequency-dependent dielectric function, $\varepsilon(\omega)$, in the limit of zero frequency. That is, $\varepsilon_s = \varepsilon(\omega \to 0)$. The numerical value of ε_s can be computed from the fluctuations of the total dipole moment of the system. The total dipole moment $\boldsymbol{M}$ is the summation of the molecular dipole moments $(\boldsymbol{\mu}_i)$, $\boldsymbol{M} = \sum_{i=1}^{N} \boldsymbol{\mu}_i$. Dipole moment for each molecule can be calculated from the charge (q) and positions $(\boldsymbol{r})$ of the corresponding atoms $(\boldsymbol{\mu}_i = \sum q_i \boldsymbol{r}_i)$. The static dielectric constant is then calculated as[38,39]

$$\varepsilon_s = 1 + \frac{\langle \boldsymbol{M}^2 \rangle - \langle \boldsymbol{M} \rangle^2}{3\epsilon_0 V k_B T}, \tag{1}$$

where ϵ_0 is vacuum permittivity, V the volume, k_B the Boltzmann constant and T the temperature. Angular brackets represent ensemble averaging. The finite system Kirkwood g-factor (G_K) describes the correlation among the molecular dipoles and connects to the total moment by the following relation.[40,41]

$$G_K = \frac{\langle \boldsymbol{M}^2 \rangle - \langle \boldsymbol{M} \rangle^2}{N\boldsymbol{\mu}^2}, \tag{2}$$

where $\boldsymbol{\mu}$ is the average dipole moment of a single molecule. Therefore, $G_K = 1$ for an arrangement of totally randomised and uncorrelated dipoles, $G_K > 1$ for configurations with the parallel alignment of dipoles, and $G_K < 1$ for antiparallel orientation of molecular dipoles at the individual level. From this finite system Kirkwood correlation factor, an infinite system Kirkwood factor (g_K) can be evaluated from the following equation.[40,41]

$$g_K = \frac{(2\varepsilon_s + 1)}{3\varepsilon_s} G_K, \tag{3}$$

Frequency-dependent dielectric spectrum is determined from the Laplace-Fourier transform of the normalised total dipole moment autocorrelation function, $\phi(t)$, which is the pulse-response function of the system.[42]

$$\phi(t) = \frac{\langle \boldsymbol{M}(0) \cdot \boldsymbol{M}(t) \rangle}{\langle |\boldsymbol{M}(0)|^2 \rangle} \tag{4}$$

Note that $\phi(t)$, by construction, starts from unity at $t = 0$ and decays to zero with time. The multi-exponential or non-exponential character of $\phi(t)$ is then reflected in the experimental DR as multi-Debye, Cole-Cole and Cole-Davidson relaxation processes. Linear response theory[43] approximates the natural dynamics of a given system to its responses in presence of an external weak electric field. Frequency-dependent dielectric spectrum is then obtained as[42]

$$\frac{\varepsilon(\omega) - 1}{\varepsilon_s - 1} = \mathcal{L}_{i\omega}\left[-\frac{d\phi(t)}{dt}\right], \tag{5}$$

where,

$$\mathcal{L}_{i\omega}[f(t)] = \int e^{i\omega t} f(t) dt. \tag{6}$$

In practice, the simulated $\phi(t)$ is fitted with a suitable fit function, $\varphi(t)$, because of the poor converging nature of $\phi(t)$. Then Laplace–Fourier transform of $\varphi(t)$ is performed (instead of $\phi(t)$) to obtain the dielectric spectrum.

Real and imaginary parts of the dielectric spectrum are defined as[44]

$$\varepsilon(\omega) = \varepsilon'(\omega) - i\varepsilon''(\omega). \tag{7}$$

There is another correlation function defining the correlation between a molecular dipole with itself. This is a self-dipole autocorrelation function and is defined as[44]

$$C_\mu(t) = \frac{\langle \boldsymbol{\mu}_i(t) \cdot \boldsymbol{\mu}_i(0) \rangle}{\langle |\boldsymbol{\mu}_i(0)|^2 \rangle}. \tag{8}$$

As for $\phi(t)$ described above, $C_\mu(t)$ is a normalised time autocorrelation function and decays with time from unity to zero.

2.2 *Computational details*

We have already mentioned that two different versions of the OPLS force fields have been employed in the present study. Note that the OPLS-UA model interaction potential employed here is not the same as the united atom version of the original OPLS model.[45] This model is appropriately tweaked to reproduce the experimental ε_s of neat molten acetamide. The functional forms of both the force fields are the same as[35,36].

$$V(r) = \sum_{\text{bonds}} K_r(r - r_{eq})^2 + \sum_{\text{angles}} K_\theta(\theta - \theta_{eq})^2 + \sum_{\text{torsions}} \left[\frac{V_1}{2}(1 + \cos\phi) + \frac{V_2}{2}(1 - \cos 2\phi) + \frac{V_3}{2}(1 + \cos 3\phi) + \frac{V_4}{2}(1 - \cos 4\phi)\right] + \sum_i \sum_{j>i} \left\{\frac{q_i q_j}{4\pi\varepsilon_0 r_{ij}} + 4\varepsilon_{ij}\left[\left(\frac{\sigma_{ij}}{r_{ij}}\right)^{12} - \left(\frac{\sigma_{ij}}{\sigma r_{ij}}\right)^{6}\right]\right\} f_{ij}. \quad (9)$$

In the above equation, K_r and K_θ are the force constants for bond stretching and angle bending respectively, r_{eq} and θ_{eq} denote the equilibrium bond-length and the angle values, and V represents the Fourier coefficient of torsional angle ϕ. r_{ij} is the distance between two atoms i and j with partial charges q_i and q_j, σ and ε are respectively the van der Waals diameter and the well-depth of the Lennard-Jones potential. Geometric combination rules for the Lennard-Jones parameters are $\sigma_{ij} = (\sigma_{ii}\sigma_{jj})^{1/2}$ and $\varepsilon_{ij} = (\varepsilon_{ii}\varepsilon_{jj})^{1/2}$. The factor $f_{ij} = 1$ except for 1-4 interactions where $f_{ij} = 0.5$.

All simulations have been performed in the GROMACS-2018.3 MD package.[46] The long-range electrostatic interactions were treated *via* the Ewald summation technique.[47] Both types of short-range interactions were truncated at 1.1 nm. A particle mesh Ewald method was used with a 0.12 nm grid and a spline of order 4.

Initial structures were built using Packmol.[48] Three systems were simulated for the OPLS-UA model interaction potential containing 250, 500, and 1000 molecules. For the OPLS-AA model also, three systems with the same number of molecules were considered. To check the impact of initial configuration, we have performed another independent MD run containing 500 molecules and using OPLS-UA force field model at the same conditions. Periodic boundary conditions were used for all the systems. NPT equilibrations were done for 20 ns (OPLS-UA) and 5 ns (OPLS-AA) at 1 bar and 358.15 K using the leap-frog algorithm with a time step of 1 fs. Note that systems using OPLS-UA potential need much more time to get equilibrated compared to OPLS-AA model. Density, temperature and pressure values are observed through the equilibration times. These values get satisfactorily converged within the mentioned equilibration times. Nosé-Hoover thermostat[49] was used for the temperature coupling with time constants 0.2 ps (OPLS-UA) and 1 ps (OPLS-AA). To couple pressure, Parrinello-Rahman barostat[50] was used with time constants 0.5 ps (OPLS-UA) and 5 ps (OPLS-AA). LINCS[51] algorithm was employed to retain all bonds constrained. Thermostat and barostat relaxation times are taken from respective references for OPLS-UA[35] and OPLS-AA.[36] Production runs (100 ns for OPLS-UA and 60 ns for OPLS-AA) were carried out using the same conditions as equilibration with output files were saving at every 100 fs. Convergence of the value of static dielectric constant with time dictates the goodness of simulation. In the case of OPLS-UA interaction potential, longer times are required for this type of convergence.

3. Results and Discussion

3.1 *Density and self-diffusion coefficients*

To check the reliability of the present simulations liquid densities from different runs have been calculated and these values are compared against the available data[35–37] in Table 1.

For clarity, we have shown here only one data set for OPLS-AA model. Density and self-diffusion coefficient values of 250 and 500 molecules for OPLS-AA model are provided in Table S1, SI. Clearly, our simulated density employing the OPLS-UA interaction matches well with the experimental value.[37] In addition, densities predicted here employing the OPLS-UA and OPLS-AA potentials are in very good agreement with the available simulated densities.[35,36] This provides us with the necessary confidence to continue with our proposed study. From the density and self-diffusion coefficient values for two independent MD runs of 500 molecules for OPLS-UA force field (will be denoted as Run 1 and Run 2 hereafter), summarized in Table S2 of Supplementary Information, no

Table 1. Density and self-diffusion coefficient for different potential models.

Force field	Model	No. of molecules	T (K)	ρ (kg m^{-3})	D ($\times$ 10^{-5} cm^2 s^{-1})
OPLS	UA[35]	250	358.15	994	0.274
		500		995.6 (998.9)	0.285
		1000		996.4	0.274
	AA[36]	1000		1024.3 (1018.7)	0.816
Drude oscillator[62]		64	373	–	–
CHARMM-PIPF[53]		256		–	0.75 ± 0.04
CHARMM[27]		512	365	–	0.91
Experiment[37]			–	998.6	–

Values are shown for the present simulation as well as from existing literatures. Values in parentheses indicate values reported in the corresponding paper

significant effect of initial configuration on these values has been detected.

The self-diffusion coefficient is representative of diffusive dynamics in a given system. The translational mean square displacements (MSDs), $\langle \left|\overrightarrow{\Delta r(t)}\right|^2 \rangle = \frac{1}{N}\langle \sum_{i=1}^{N} \left|\overrightarrow{r}_i^c(t) - \overrightarrow{r}_i^c(0)\right|^2 \rangle$, have been followed and the diffusion coefficients,[52] $D = \left[\frac{1}{6}(\langle \left|\overrightarrow{\Delta r(t)}\right|^2 \rangle\right]_{t\to\infty}$, for molten acetamide have been estimated from the present simulations. The simulated self-diffusion coefficients for our systems and a comparison with the available data are also provided in Table 1. D values shown in the last column of Table 1 suggest that the system size dependence for the OPLS-UA system is negligible. Also, a negligible system size dependence has been observed for OPLS-AA model (Table S1, SI). However, the OPLS-UA predicted diffusion coefficient is $\sim$3 times slower than that provided by the OPLS-AA interaction parameters. Interestingly, the OPLS-AA predicted diffusion coefficient for molten acetamide agrees well with those predicted by the CHARMM-PIPF[53] and CHARMM[27] interaction potentials. In addition, the diffusion coefficient predicted here by the OPLS-AA potential ($\sim$0.82 $\times$10^{-5} cm^2 s^{-1}) is in good agreement with that (0.92 $\times$ 10^{-5} cm^2 s^{-1}) reported in the quasi-elastic neutron scattering (QENS) measurements.[27] It is therefore likely that DR time constants obtained by employing the OPLS-AA interaction potential for liquid acetamide would be in better agreement with experiments than those predicted via the OPLS-UA interaction potential.

3.2 *Radial distribution functions (RDFs)*

The structure of liquids in two dimensions can be visualized by the RDFs which describe the probability of finding a particle at a distance r from a tagged particle. It is calculated using the following equation:

$$g_{ij}(r) = \frac{1}{\rho N}\left\langle \sum_{ij} \delta(r - r_{ij}) \right\rangle \tag{10}$$

where ρ is the number density, N is the total number of particles and i and j are particle indices where angular brackets denote ensemble average.

Computed RDFs for liquid acetamide are displayed in Figure 1 for distributions of different atoms in the system. It has been already suggested that H-bond plays an important role in the structure and dynamics of liquid acetamide.[54–59] Calculated RDFs between different types of particles for the present systems depict the liquid structure (in two dimensions though) and provide scope to compare between the predictions by these two potential models.

The upper-left panel of Figure 1 shows the RDF of N (-CONH$_2$)-O (-CONH$_2$). We can see that there is no system size dependence. For both of the models, the first peak appears at $\sim$2.85 Å which is similar to earlier reports.[45,53,60] This peak is mainly the result of hydrogen bonding as explained in Ref [36]. The first peak height is greater for the OPLS-UA model predicted RDF than that by the OPLS-AA model. This may be a reflection of a relatively stronger H-bond interaction in the OPLS-UA acetamide and can partially explain the relatively lower diffusion coefficient value.

The upper-right panel represents O (-CONH$_2$)-H (-CONH$_2$) RDFs for acetamide. From the X-ray diffraction study,[12,61] O (-CONH$_2$) —H (-CONH$_2$) bond length is found as 3.03 Å which is comparable with the first peak minimum of the corresponding RDF shown here. The appearances of peak positions are consistent with previous studies,[45,53,60] suggesting that the underlying liquid structure remains the same in the present simulations as found in previous studies.[45,53,60]

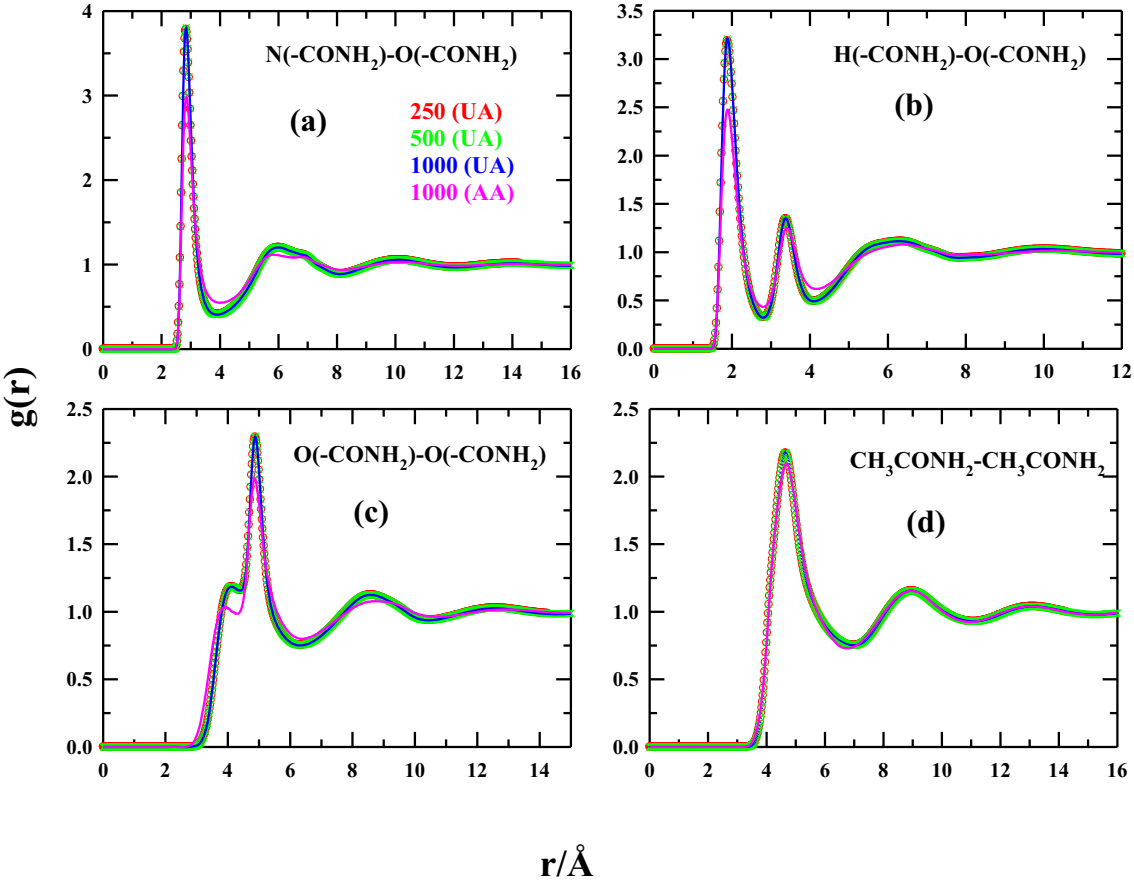

Figure 1. Simulated radial distribution functions (RDFs) for different atom-sites of acetamide molecules are shown in four panels. Following site-site RDFs are presented: (**a**) N(-$CONH_2$)-O(-$CONH_2$), (**b**) H(-$CONH_2$)-O(-$CONH_2$), (**c**) O(-$CONH_2$)-O(-$CONH_2$), (**d**) centre-of-mass of acetamide molecules. Representations are colour defined as described in panel (**a**).

Here also the first peak height for the OPLS-UA model is greater than that for the OPLS-AA model.

An interesting feature is observed for O (-$CONH_2$)-O (-$CONH_2$) RDFs, shown in the lower-left panel of this figure. Notice that a shoulder appears prior to the main peak. The main peak indicates the configuration where two O atoms of two different molecules approach and a hydrogen atom of one of the two molecules resides between them. The shoulder depicts a spatial arrangement when no hydrogen atom resides between them. The lower-right panel depicts the centre-of-mass RDFs of acetamide molecules.

3.3 *Static dielectric properties*

The calculation of the static dielectric constant serves two purposes. Apart from providing insights about the collective orientational structure of the dipolar liquid, convergence for the simulated ε_s with time to a constant value indicates whether the simulation is long enough for calculating the dynamic dielectric properties. We have estimated ε_s for the neat liquid acetamide and the Kirkwood g-factor (for finite and infinite systems). Figure 2 depicts the fluctuations of the simulated ε_s with time and its convergence to a certain value after a sufficiently long duration.

Notice that the simulated ε_s fluctuates more when the system size is relatively small. Interestingly, the OPLS-AA model interaction potential predicts an ε_s value nearly half of that by the OPLS-UA model, although the extent of the time-dependent fluctuations is much less for the OPLS-AA predicted ε_s and the convergence is achieved much faster. In addition, a choice of 100 ns production run-time in the present work appears to be logical for simulations of DR in neat molten acetamide.

Table 2 summarizes the ε_s values simulated in the present work and compares with those from earlier simulations employing different model interaction potentials[35,36,53,62] and the relevant measurements.[26,37] Comparison of various static dielectric properties

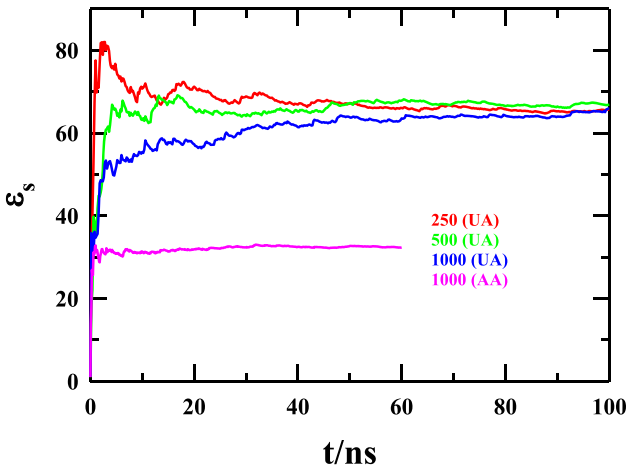

Figure 2. Evolutions of static dielectric constant with simulation time for all systems. All systems are fairly converged within the simulation run time. Each system is uniquely colour-defined.

among systems with different sizes using OPLS-AA model are provided in Table S3, SI. The same properties can be found for Run 1 and Run 2 in Table S4, SI. Clearly, the variation is tiny and thus system size dependence is negligible.

Clearly, the OPLS-UA[35] model provides a much better description of the experimental ε_s than by the OPLS-AA[36] ($\varepsilon_s \sim$ 32) and the CHARMM-PIPF[53] ($\varepsilon_s \sim$ 154) interaction potential. Note the Drude oscillator model[62] is quite successful in predicting the experimental ε_s for liquid acetamide. The estimated values for the average dipole moment and the finite Kirkwood g-factor (G_K) by the Drude oscillator model also corroborate well with the OPLS-UA predictions. The OPLS-AA model, however, substantially underestimates the orientational structure of the liquid acetamide because the estimated ε_s and the Kirkwood factors (G_K and g_K) are significantly lower than those predicted by the other interaction potentials. While stating so we keep in mind that (i) a G_K value greater than unity implies a strong correlation among the molecular dipoles and (ii) the numerical value of ε_s is connected to the macroscopic total orientational pair correlation function (h^{110}) by the relation,[63] $\frac{(\varepsilon_s-1)(2\varepsilon_s+1)}{9\epsilon_0 y} = 1 + \frac{4\pi\rho}{3}\int_0^\infty r^2 h^{110}(r)dr$, where the polarity parameter, $y = 4\pi\mu^2\rho/9k_BT$, ρ being the number density. Next, we compare the performance of the OPLS-UA and OPLS-AA interaction potentials in predicting the measured DR timescales.

3.4 *Dynamic dielectric properties*

Monitoring the correlation among dipoles with time, the dipole moment autocorrelation function, provides an insight into the relaxation dynamics of the system. Two different autocorrelation functions have been calculated in this work. They are the total dipole moment autocorrelation function, $\phi(t)$, and the self-dipole moment autocorrelation function, $C_\mu(t)$. While the total dipole moment autocorrelation function tracks the collective orientational relaxations and thus provides a direct theoretical description of the experimentally measured DR data, the self-dipole moment autocorrelation function treats the dipolar orientations at the single-molecule level and explores the connection between the individual dipolar rotational dynamics and the collective orientational polarization relaxations.

The upper panel of Figure 3 presents the time dependence of the simulated total dipole moment autocorrelation function, $\phi(t)$, for the neat liquid acetamide interacting via the OPLS-UA and OPLS-AA potentials. The system size dependence (studied for the OPLS-UA interactions) is negligible. The corresponding results for OPLS-AA model containing a different number of molecules are shown in Figure S1 and fit parameters are provided in Tables S5 and S6 of Supplementary Information. Here also no significant system size dependence is detected. The

Table 2. Static dielectric properties for different potential models.

Force field	Model	No. of molecules	T(K)	ε_s	G_K	g_K	$\langle\mu\rangle$(D)
OPLS	UA[35]	250	358.15	65.6	2.31	1.55	5.71
		500		66.8	2.34	1.57	
		1000		65.9	2.31	1.55	
	AA[36]	1000		32.3	1.95	1.32	4.26
Drude oscillator[62]		64	373	66 ± 3	2.4 ± 0.2	–	5.80
CHARMM-PIPF[53]		256		154	–	–	5.30
Experiment[26]			354	66	—	–	–
Experiment[37]			–	68.2	—	–	–

Values are shown for the present simulation as well as from existing literatures.

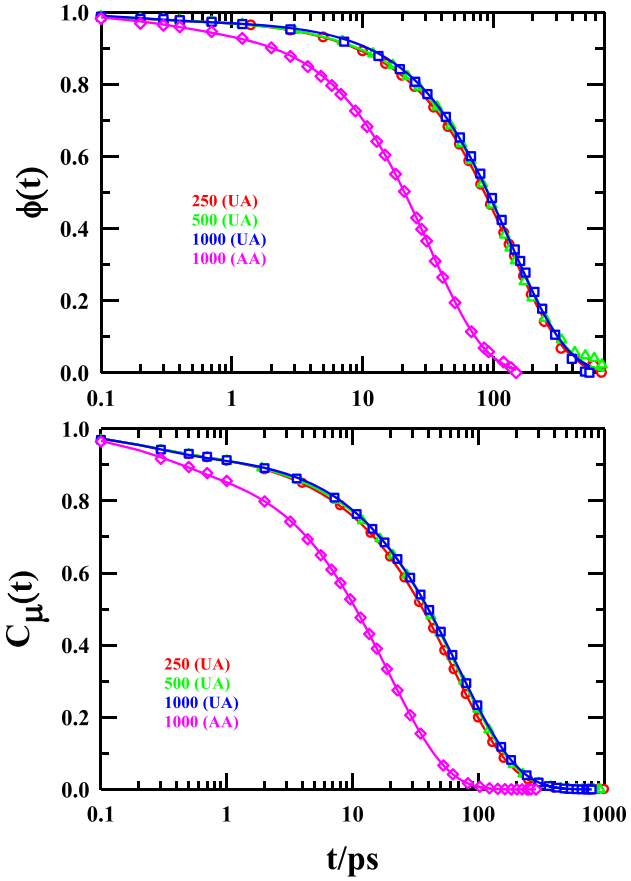

Figure 3. Simulated decays of total dipole moment autocorrelation function (upper panel) and dipole moment autocorrelation function for single molecules (lower panel) of all systems. Each system is uniquely colour-defined. Open symbols are simulated data points and solid lines denote corresponding fits.

relaxation for $\phi(t)$ obtained by employing the OPLS-AA potential is much faster than that predicted by the OPLS-UA interactions. The lower panel of Figure 3 shows the time-dependent decay of the self-dipole moment autocorrelation function, $C_\mu(t)$. The dependence of $C_\mu(t)$ on the interaction potential and the system size is the same as that found for $\phi(t)$. Parameters obtained via multi-exponential fits to the simulated $\phi(t)$ decays are summarized in Table 3. Experimentally measured DR times and amplitudes are also shown in this table to facilitate a comparison between simulations and experiments. Table 4 summarizes the fit parameters required to adequately describe the simulated $C_\mu(t)$ decays. Plots of $\phi(t)$ and $C_\mu(t)$ for Run 1 and Run 2 are provided in Figure S2, SI. Fit parameters are summarized in Tables S7 and S8, SI, respectively. These results suggest tiny effects of starting structures on final results.

From the data summarized in Table 3, it is evident that none of these two model interaction potentials can correctly reproduce the slowest experimental DR time constants, although the amplitude associated with it is predicted nearly quantitatively. The slowest DR time constant predicted by the OPLS-UA model is $\sim$2.5 times slower than that reported in experiments, whereas the OPLS-AA predicted timescale is $\sim$1.7 times faster than in experiments. The degree of disagreement between the predicted slowest DR times by these two versions of the OPLS model potentials (a factor of $\sim$4) is reflective of that already observed between the translational diffusion coefficients. The other slower time constant, which is in the sub-10 ps regime in experiments, is missing for the OPLS-UA interaction when the system size is the largest. In fact, the OPLS-AA system studied here also does not predict the sub-10 ps timescale. The other sub-picosecond timescale predicted in simulations for both the interactions is absent in experiments. This is because the limited frequency window ($0.2 \leq \nu/GHz \leq 50$) employed in those measurements cannot detect dynamics faster than a couple of picoseconds and thus completely misses the relaxation contributions arising from the collective solvent modes such as the intermolecular vibrations and librations of extensively H-bonded systems of liquids like acetamide.

The self-dipole autocorrelation function, $C_\mu(t)$, maps the correlation between a single dipole with itself at different time lags and therefore tracks the dynamics at the single-molecule level. Parameters obtained from fits to $C_\mu(t)$ decays are shown in Figure 3 (lower panel) are summarized in Table 4.

Notice the weakly stretched exponential behaviour of the slowest relaxation component of the $C_\mu(t)$ decays. This is a reflection of the non-Debye behaviour of liquid acetamide and will emerge again when we show later the dielectric response *via* Cole-Cole plots. As expected, the slowest decay time constant for $C_\mu(t)$ predicted by the OPLS-UA model is $\sim$3 times slower than that by the OPLS-AA interactions. Interestingly, the sub-10 ps and the sub-picosecond timescales are present in all the $C_\mu(t)$ decays simulated. The similarity in decay amplitudes between the $C_\mu(t)$ and the $\phi(t)$ relaxations strongly suggests that the collective orientational polarization relaxation is intimately connected to the single dipole orientation dynamics. Note this single dipole orientation relaxation ($C_\mu(t)$), although describes orientation dynamics of single molecular dipoles, is collective in nature because this molecular dipole orientational relaxation occurs in a potential created by its surrounding neighbours.

Table 3. Fit parameters for total dipole moment autocorrelation functions for all systems.

Model	No of molecules	a_1	τ_1 (ps)	a_2	τ_2 (ps)	a_3	τ_3 (ps)	$\langle\tau\rangle$(ps)
UA	250	0.96	130.6	0.02	4.4	0.02	0.1	125.5
	500	0.96	138	0.02	4	0.02	0.1	132.6
	1000	0.98	135.5	–	–	0.02	0.2	132.8
AA	1000	0.96	32	–	–	0.04	0.3	30.7
Experiment[26]		0.97	55	0.03	5.5	–	–	53.5

For systems containing 250 and 500 molecules, tri-exponential fit functions are used and for systems of 1000 molecules bi-exponential functions are fitted. Experimental results are for two-Debye fitting of experimental DR spectra taken from Ref. 26.

Table 4. Fit parameters for dipole moment autocorrelation function for single molecules.

Model	No. of molecules	a_1	τ_1 (ps)	β	a_2	τ_2 (ps)	a_3	τ_3 (ps)	τ_{long}* (ps)	$\langle\tau\rangle$(ps)
UA	250	0.91	63.3	0.92	0.03	2.8	0.06	0.2	65.8	60
	500	0.91	68.5	0.93	0.03	3.5	0.06	0.2	70.4	64.2
	1000	0.90	71	0.93	0.03	4.3	0.07	0.2	73.4	66.2
AA	1000	0.79	21.4	1.00	0.11	6.2	0.10	0.3	21.4	17.6

In the case of UA model systems combination of stretched exponential and bi-exponential is used whereas for AA model system tri-exponential function is fitted

$^*\tau_{long} = \frac{\tau\Gamma(\beta^{-1})}{\beta}$

3.5 *Dielectric spectra*

Following the method described in section 2.1, dielectric spectra for different systems have been calculated in the frequency range of $0.001 \leq \nu/GHz \leq 10^5$. The existing experimental spectra[26] has been recorded in the frequency window $0.2 \leq \nu/GHz \leq 50$. Therefore, the available experimental DR spectra have been regenerated using the fit functions given in Table 3 in order to facilitate a comparison between the simulations and experiments.

Figure 4 presents the real (upper panel) and the imaginary (lower panel) components of the simulated dielectric relaxation spectra employing both the model interaction potentials and compares them with those from experiments. As ε_∞ and ε_s vary for different cases, the spectra are compared after appropriate normalization. It may be noted in both the panels that the experimental spectra are flanked by the simulated counterparts where the OPLS-UA predictions are shifted to lower and OPLS-AA predictions to higher frequencies with respect to the experiments. This means that the relaxation predicted by the OPLS-AA model potential is faster than experiments while the same predicted by the OPLS-UA parameters is slower than what has been found in measurements. This is exactly what we have already seen while comparing $\phi(t)$ relaxation timescales with those from experiments. Notice also that there is no significant system size dependence in spectra simulated by employing the OPLS-UA interaction potential.

Figure 5 displays the Cole-Cole plots for different systems simulated. For Debye liquids, the Cole-Cole plot is a perfect semi-circle.[44] Thus, the non-Debye nature of DR in liquid acetamide is reflected by the small deviation (from being a perfect semi-circle) shown by both the simulated and experimental spectra. Tiny semicircles that appeared at the high-frequency region for MD simulation are due to the fast relaxation process which has been missed in the experiments because of the limited frequency window. The non-Debye behaviour of molten acetamide has also been found while following the collective single-particle reorientational relaxations.[64,65]

4. Conclusions

We present here for the first time a detailed comparison between the experimental and simulated dielectric relaxation spectra of neat molten acetamide where the role of single dipolar orientation dynamics in the collective polarization relaxation has been investigated and understood. This work also assumes importance when one considers that no simulation study of DR in molten acetamide was available although a number of

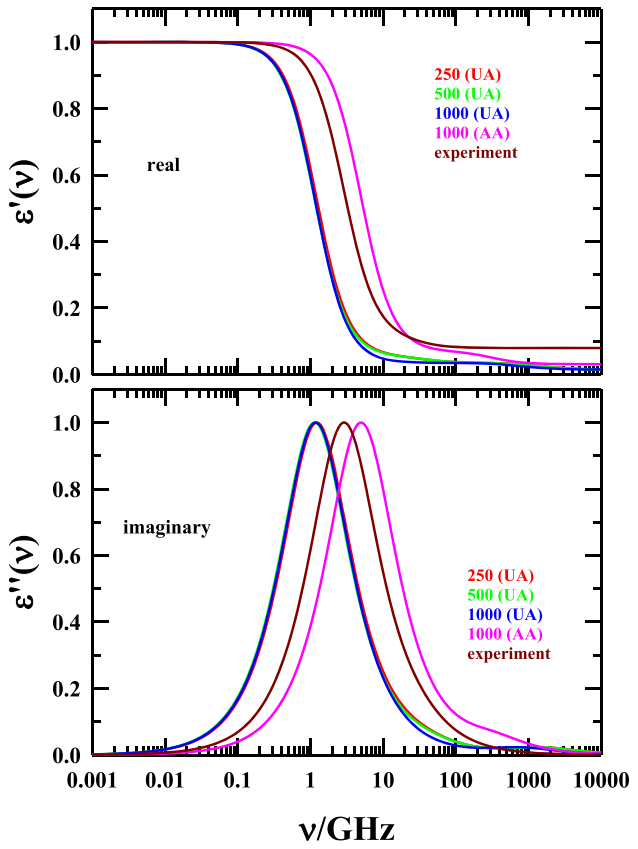

Figure 4. Real (upper panel) and imaginary (lower panel) parts of normalized dielectric relaxation spectra obtained from simulation for all acetamide systems are represented along with experimental results (Ref. 26). DRS data for the experiment is reproduced using existing fit parameters reported in literature. Each system is uniquely colour-defined.

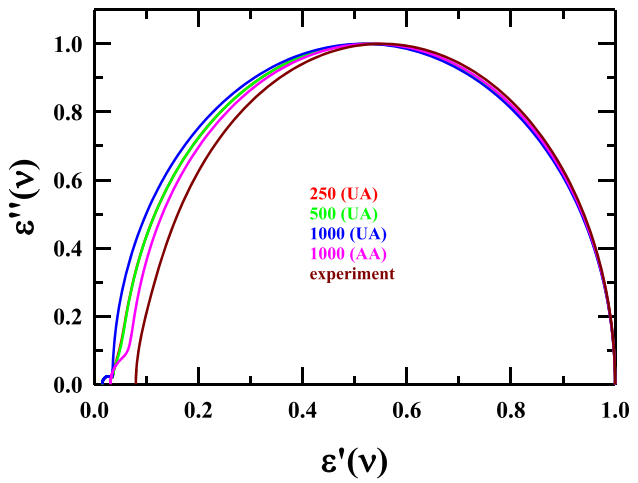

Figure 5. Cole-Cole plot of the frequency-dependent dielectric function. Simulation, as well as experimental results (reproduced from fit parameters of Ref. 26), are shown. Each system is uniquely colour-defined.

model interaction potentials were developed to predict various solvent properties and translational diffusion coefficients of liquid acetamide. The study of system size dependence of DR for liquid acetamide conducted here, although limited within a model potential, brings out useful information regarding the sufficiency of system size for performing simulations of H-bonded dipolar liquids such as liquid acetamide. The Cole-Cole plot correctly hints at the non-Debye behaviour of acetamide already found in simulation studies of reorientational relaxations. The results obtained here will be useful for simulation study DR in acetamide containing deep eutectic solvents, particularly for the investigation of the mega-value of the static dielectric constant of ionic acetamide deep eutectics and the corresponding relaxation time constants reported in the KHz-MHz measurements performed earlier. Moreover, the comparison between the simulation results obtained by employing the OPLS-AA and OPLS-UA potentials shown in this work will be an important guide for making a logical choice of interaction potential while planning a study on dielectric properties of acetamide containing multi-component mixtures.

Acknowledgements

Mr. D. Maji gratefully acknowledges the DST-INSPIRE, Government of India for granting a research fellowship.

Supplementary Information (SI)

Calculated thermodynamic, dynamic, and dielectric properties of OPLS-AA systems containing 250, and 500 molecules are provided in Supplementary Information (SI). Various properties calculated from two independent runs for OPLS-UA systems and 500 acetamide molecules are also reported in this SI which is available at www.ias.ac.in/chemsci.

References

1. Mitchell J B O and Price S L 1989 On the electrostatic directionality of N-H···O=C hydrogen bonding *Chem. Phys. Lett.* **154** 267
2. Dixon D A, Dobbs K D and Valentini J J 1994 Amide-water and amide-amide hydrogen bond strengths *J. Phys. Chem.* **51** 13435
3. Ludwig R, Weinhold F and Farrar T C 1997 Theoretical study of hydrogen bonding in liquid and gaseous N-methylformamide *J. Chem. Phys.* **107** 499
4. Krestyaninov M A, Odintsova E G, Kolker A M and Kiselev M G 2018 The structure of water – acetamide hydrogen bonded complexes. Quantum chemical analysis *J. Mol. Liq.* **264** 343

5. Wong M W and Wiberg K B 1992 Structure of acetamide: Planar or nonplanar *J. Phys. Chem.* **96** 668
6. Wallace R A 1971 Equivalent conductivity of potassium halides in molten acetamide *J. Phys. Chem.* **75** 2687
7. Dawson L R, Sears P G and Graves R H 1955 Solvents having high dielectric constants. II. Solutions of alkali halides in N-Methylacetamide from 30 to 60° *J. Am. Chem. Soc.* **77** 1986
8. Yntema L F and Audrieth L F 1930 Acetamide and formamide as solvents for the electrodeposition of metals *J. Am. Chem. Soc.* **52** 2693
9. Stafford O F 1933 Acetamide as solvent *J. Am. Chem. Soc.* **55** 3987
10. Kerridge D H 1988 The chemistry of molten acetamide and acetamide complexes *Chem. Soc. Rev.* **17** 181
11. Nasr S, Ghédira M and Cortés R 1999 H-bonding in liquid acetamide as studied by X-ray scattering *J. Chem. Phys.* **110** 10487
12. Nasr S 2001 H-bonding in amorphous acetamide CH_3CONH_2 as studied by X-ray scattering *J. Chem. Phys.* **115** 6569
13. Trabelsi S and Nasr S 2004 Intermolecular association in liquid N-methylacetamide as studied by X-ray scattering *J. Chem. Phys.* **121** 6380
14. Hammami F, Nasr S and Bellissent-Funel M-C 2005 Neutron scattering study of the H-bond network in amorphous N-methylformamide *J. Chem. Phys.* **122** 064505
15. Trabelsi S, Bahri M and Nasr S 2005 X-ray scattering and density functional calculations to study the presence of hydrogen bonded clusters in liquid N-methylacetamide *J. Chem. Phys.* **122** 024502
16. Kashyap H K, Pradhan T and Biswas R 2006 Limiting ionic conductivity and solvation dynamics in formamide *J. Chem. Phys.* **125** 174506
17. Pattanayak S K, Prashar N and Chowdhuri S 2011 Effect of temperature and pressure on the structure, dynamics and hydrogen bond properties of liquid N-methylacetamide: A molecular dynamics study *J. Chem. Phys.* **134** 154506
18. Biswas R and Bagchi B 1996 Solvation dynamics in slow viscous liquids: Application to amides *J. Phys. Chem.* **100** 1238
19. Das S, Biswas R and Mukherjee B 2015 Reorientational jump dynamics and its connections to hydrogen bond relaxation in molten acetamide: An all-atom molecular dynamics simulation study *J. Phys. Chem. B* **119** 274
20. Srinivasan H, Sharma V K, Mitra S, Biswas R and Mukhopadhyay R 2019 Dynamics in acetamide+$LiNO_3$ deep eutectic solvents *Phys. B Cond. Matter* **562** 13
21. Das A, Das S and Biswas R 2013 Fast fluctuations in deep eutectic melts: Multi-probe fluorescence measurements and all-atom molecular dynamics simulation study *J. Chem. Phys.* **581** 47
22. Guchhait B, Daschakraborty S and Biswas R 2012 Medium decoupling of dynamics at temperatures $\sim$100 K above glass-transition temperature: A case study with (acetamide + lithium bromide/nitrate) melts *J. Chem. Phys.* **136** 174503
23. Pal T and Biswas R 2011 Heterogeneity and viscosity decoupling in (acetamide+electrolyte) molten mixtures: A model simulation study *Chem. Phys. Lett.* **517** 180
24. Mukherjee K, Das S, Tarif E, Barman A and Biswas R 2018 Dielectric relaxation in acetamide + urea deep eutectics and neat molten urea: Origin of time scales via temperature dependent measurements and computer simulations *J. Chem. Phys.* **149** 124501
25. Das S, Biswas R and Mukherjee B 2015 Orientational jumps in (acetamide + electrolyte) deep eutectics: Anion dependence *J. Phys. Chem. B* **119** 11157
26. Mukherjee K, Das A, Choudhury S, Barman A and Biswas R 2015 Dielectric relaxations of (acetamide + electrolyte) deep eutectic solvents in the frequency window, $0.2 \leq \nu/\mathrm{GHz} \leq 50$: Anion and cation dependence *J. Phys. Chem. B* **119** 8063
27. Srinivasan H, Sharma V K, García Sakai V, Embs Jan P, Mukhopadhyay R and Mitra S 2020 Transport mechanism of acetamide in deep eutectic solvents *J. Phys. Chem. B* **124** 1509
28. Laage D and Hynes J T 2006 A molecular jump mechanism of water reorientation *Science* **311** 832
29. Laage D and Hynes J T 2008 On the molecular mechanism of water reorientation *J. Phys. Chem. B* **112** 14230
30. Amoco A, Berchiesi G, Cametti C and Di Biasio A 1987 Dielectric relaxation of an acetamide-sodium thiocyanate eutectic mixture *J. Chem. Soc. Faraday Trans.* **2(83)** 619
31. Berchiesi G, De Angelis M, Rafaiani G and Vitali G 1992 Electrolyte-acetamide molten mixtures *J. Mol. Liq.* **51** 11
32. Berchiesi G 1999 Structural microheterogeneity and evidence of cooperative movement of charges in molten acetamide-electrolyte mixtures *J. Mol. Liq.* **83** 271
33. Berchiesi G, Vitali G and Amico A 1986 Ultrasonic and viscoelastic relaxation in molten eutectic acetamide-$LiNO_3$ *J. Mol. Liq.* **32** 99
34. Berchiesi G, Farhat F, De Angelis M and Barocci S 1992 High dielectric constant supercooled liquids, tools in energetic problems *J. Mol. Liq.* **54** 103
35. Pineda J A A, Maldonado G A M, Rojas E N and Alejandre J 2015 Parametrisation of a force field of acetamide for simulations of the liquid phase *Mol. Phys.* **113** 2716
36. Caleman C, van Maaren P J, Hong M, Hub J S, Costa L T and van der Spoel D 2012 Force field benchmark of organic liquids: Density, enthalpy of vaporization, heat capacities, surface tension, isothermal compressibility, volumetric expansion coefficient, and dielectric constant *J. Chem. Theory Comput.* **8** 61
37. Lide D R 2009 In *CRC Handbook of Chemistry and Physics* (Cleveland: CRC Press)
38. Neumann M 1983 Dipole moment fluctuation formulas in computer simulations of polar systems *Mol. Phys.* **50** 841
39. Froehlich H 1958 In *Theory of Dielectrics* (New York: Oxford University Press)
40. Kirkwood J G 1939 The dielectric polarization of polar liquids *J. Chem. Phys.* **7** 911

41. Neumann M 1986 Dielectric relaxation in water. Computer simulations with the TIP4P potential *J. Chem. Phys.* **85** 1567
42. Neumann M and Steinhauser O 1983 On the Calculation of the frequency-dependent dielectric constant in computer simulations *Chem. Phys. Lett.* **102** 508
43. Kubo R 1966 The fluctuation-dissipation theorem *Rep. Prog. Phys.* **29** 255
44. Boettcher C J F and Bordewijk P 1978 In *Theory of Electric Polarization II* (Amsterdam: Elsevier)
45. Jorgensen W L, Maxwell D S and Rives J T 1996 Development and testing of the OPLS all-atom force field on conformational energies and properties of organic liquids *J. Am. Chem. Soc.* **118** 11225
46. Berendsen H J C, van der Spoel D and van Drunen R 1995 GROMACS: A message-passing parallel molecular dynamics implementation *Comp. Phys. Commun.* **91** 43
47. Allen M P and Tildesley D J 1987 In *Computer Simulations of Liquids* (Oxford University Press: New York)
48. Martinez L, Andrade R, Birgin E G and Martinez J M 2009 Packmol: A package for building initial configurations for molecular dynamics simulations *J. Comput. Chem.* **30** 2157
49. Nosé S 1984 A unified formulation of the constant temperature molecular dynamics methods *J. Chem. Phys.* **81** 511
50. Parrinello M and Rahman A 1981 Polymorphic transitions in single crystals: A new molecular dynamics method *J. Appl. Phys.* **52** 7182
51. Hess B, Bekker H, Berendsen H J C and Fraaije J G E M 1997 LINCS: A linear constraint solver for molecular simulations *J. Comput. Chem.* **18** 1463
52. Hansen J P and McDonald I R 1986 In *Theory of Simple Liquids* (Cambridge: Academic Press)
53. Xie W, Pu J, MacKerell A D Jr and Gao J 2007 Development of a polarizable intermolecular potential function (PIPF) for liquid amides and alkanes *J. Chem. Theory Comput.* **3** 1878
54. Triggs N E and Valentini J J 1992 An investigation of hydrogen bonding in amides using Raman spectroscopy *J. Phys. Chem.* **96** 6922
55. Whitfield T W, Martyna G J, Allison S, Bates S P, Vass H and Crain J 2006 Structure and hydrogen bonding in neat N-methylacetamide: Classical molecular dynamics and Raman spectroscopy studies of a liquid of peptidic fragments *J. Phys. Chem. B* **110** 3624
56. Kuduva S S, Blaser D, Boese R and Desiraju G R 2001 Crystal engineering of primary cubanecarboxamides. Repetitive formation of an unexpected N $-$H $\cdots$ O hydrogen-bonded network *J. Org. Chem.* **66** 1621
57. Ludwig R 2000 Cooperative hydrogen bonding in amides and peptides *J. Mol. Liq.* **84** 65
58. Ludwig R, Weinhold F and Farrar T C 1997 Theoretical study of hydrogen bonding in liquid and gaseous N – methylformamide *J. Chem. Phys.* **107** 499
59. Etter M C 1990 Encoding and decoding hydrogen-bond patterns of organic compounds *Acc. Chem. Res.* **23** 120
60. Das S, Mukherjee B and Biswas R 2017 Microstructures and their lifetimes in acetamide/electrolyte deep eutectics: Anion dependence *J. Chem. Sci.* **129** 939
61. Jeffrey G A, Ruble J R, McMullan R K, DeFrees D J, Binkley J S and Pople J A 1980 Neutron diffraction at 23 K and ab initio molecular-orbital studies of the molecular structure of acetamide *Acta Crystallogr. B* **36** 2292
62. Harder E, Anisimov V M, Whitfield T, MacKerell A D Jr and Roux B 2008 Understanding the dielectric properties of liquid Amides from a polarizable force field *J. Phys. Chem. B* **112** 3509
63. Gray C G and Gubbins K E 1984 In *Theory of Molecular Fluids* (New York: Oxford University Press)
64. Das S, Biswas R and Mukherjee B 2016 Collective dynamic dipole moment and orientation fluctuations, cooperative hydrogen bond relaxations, and their connections to dielectric relaxation in ionic acetamide deep eutectics: Microscopic insight from simulations *J. Chem. Phys.* **145** 084504
65. Banerjee S, Ghorai P K, Das S, Rajbangshi J and Biswas R 2020 Heterogeneous dynamics, correlated time and length scales in ionic deep eutectics: Anion and temperature dependence *J. Chem. Phys.* **153** 234502